



Cite this: *Dalton Trans.*, 2015, 44, 15690

Hydrolysis of the RNA model substrate catalyzed by a binuclear Zr^{IV}-substituted Keggin polyoxometalate†

Thi Kim Nga Luong,^a Gregory Absillis,^a Pavletta Shestakova^{a,b} and Tatjana N. Parac-Vogt^{*a}

The reactivity and solution behaviour of the binuclear Zr^{IV}-substituted Keggin polyoxometalate (Et₂NH₂)₈{(α-PW₁₁O₃₉Zr(μ-OH)(H₂O))₂·7H₂O (ZrK 2 : 2) towards phosphoester bond hydrolysis of the RNA model substrate 2-hydroxypropyl-4-nitrophenyl phosphate (HPNP) was investigated at different reaction conditions (pD, temperature, concentration, and ionic strength). The hydrolysis of the phosphoester bond of HPNP, followed by means of ¹H NMR spectroscopy, proceeded with an observed rate constant, $k_{\text{obs}} = 11.5(\pm 0.42) \times 10^{-5} \text{ s}^{-1}$ at pD 6.4 and 50 °C, representing a 530-fold rate enhancement in comparison with the spontaneous hydrolysis of HPNP. ¹H and ³¹P NMR spectra indicate that at these reaction conditions the only products of hydrolysis are *p*-nitrophenol and the corresponding cyclic phosphate ester. The pD dependence of k_{obs} exhibits a bell-shaped profile, with the fastest rate observed at pD 6.4. The formation constant ($K_f = 455 \text{ M}^{-1}$) and catalytic rate constant ($k_c = 42 \times 10^{-5} \text{ s}^{-1}$) for the HPNP–ZrK 2 : 2 complex, activation energy (E_a) of $63.35 \pm 1.82 \text{ kJ mol}^{-1}$, enthalpy of activation (ΔH^\ddagger) of $60.60 \pm 2.09 \text{ kJ mol}^{-1}$, entropy of activation (ΔS^\ddagger) of $-133.70 \pm 6.13 \text{ J mol}^{-1} \text{ K}^{-1}$, and Gibbs activation energy (ΔG^\ddagger) of $102.05 \pm 0.13 \text{ kJ mol}^{-1}$ at 37 °C were calculated from kinetic experiments. Binding between ZrK 2 : 2 and the P–O bond of HPNP was evidenced by the change in the ³¹P chemical shift and signal line-broadening of the ³¹P atom in HPNP upon addition of ZrK 2 : 2. Based on ³¹P NMR experiments and isotope effect studies, a mechanism for HPNP hydrolysis in the presence of ZrK 2 : 2 was proposed.

Received 1st June 2015,
Accepted 30th July 2015

DOI: 10.1039/c5dt02077h

www.rsc.org/dalton

Introduction

Polyoxometalates (POMs) are generally described as a large class of inorganic oxoclusters that contain early transition metals (V, Nb, Ta, Mo and W) in their highest oxidation state. POMs have applications in a broad range of research domains including material science,^{1,2} medicine³ and catalysis.^{4,5} Recently our group discovered that a series of Zr^{IV}-substituted POM complexes could act as artificial phosphoesterases. Zr^{IV} is ideally suited as an active center in artificial hydrolytic metalloenzymes because of its high Lewis-acidity and oxophilic properties, allowing both the coordination and activation of the substrate and nucleophile. Model DNA compounds such as 4-nitrophenyl phosphate (NPP) and bis-4-nitrophenyl phosphate (BNPP) are often used when testing the

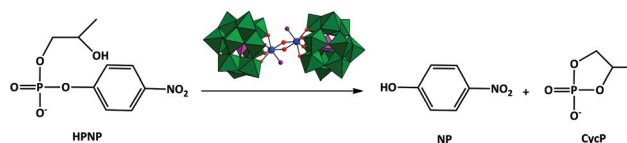
reactivity of newly developed artificial phosphatases and nucleases.^{6–12} The advantage of these model DNA substrates is the presence of good leaving groups in their structures, increasing their reactivity in comparison to for example DNA and RNA biomolecules. Phosphoester bond hydrolysis in RNA is an intramolecular transesterification, supported by the attack of the 2'-OH group to the phosphate backbone. As a result, RNA is hydrolyzed faster than DNA, which lacks such internal nucleophile. Because of the presence of an OH-group 2-hydroxypropyl-4-nitrophenylphosphate (HPNP, Scheme 1) is often used as a RNA model substrate to test the reactivity of new artificial nucleases.^{13,14}

A mononuclear Zr^{IV}-substituted Wells–Dawson type POM K₁₅H[Zr(α-P₂W₁₇O₆₁)₂].25H₂O was demonstrated to be able to

^aDepartment of Chemistry, KU Leuven, Celestijnenlaan 200F, 3001 Leuven, Belgium.
E-mail: Tatjana.Vogt@chem.kuleuven.be; <http://www.chem.kuleuven.be/lbc/>

^bNMR Laboratory, Institute of Organic Chemistry with Centre of Phytochemistry, Bulgarian Academy of Sciences, Acad. G. Bontchev Str., B1.9, 1113 Sofia, Bulgaria

† Electronic supplementary information (ESI) available: Data on the percentage of HPNP as a function of the reaction time, ³¹P NMR spectrum, kinetic data on the influence of pD, temperature. See DOI: 10.1039/c5dt02077h



Scheme 1 Hydrolysis of HPNP promoted by ZrK 2 : 2.



catalytically enhance the hydrolysis rate of the DNA model compound NPP by nearly two orders of magnitude.⁸ In a previous study we also found that the dinuclear Zr^{IV}-substituted Keggin type POM (Et₂NH₂)₈[α -PW₁₁O₃₉Zr(μ -OH)(H₂O)]₂·7H₂O (ZrK 2 : 2, Fig. 1) efficiently promoted hydrolysis of the extremely stable phosphodiester BNPP, with a 320-fold rate enhancement in comparison with spontaneous hydrolysis.¹² In addition, it was shown that the monomeric [α -PW₁₁O₃₉Zr(μ -OH)(H₂O)]⁴⁻ (ZrK 1 : 1) species is present in aqueous solution at near-neutral pD and that this species is responsible for the hydrolysis of the phosphoester bond in BNPP.⁶ ZrK 1 : 1 is considered to be more catalytically active when compared to ZrK 2 : 2 as its Zr(IV) ion has more coordinated water molecules that can be replaced by the substrate or that can act as a nucleophile. Theoretical studies have shown that when ZrK 1 : 1 interacts with NPP or BNPP, it prefers to form monodentate complexes which are more stable than the corresponding bidentate complexes.⁶

Although natural nuclease enzymes play a critical role in various biotechnology applications, efficient artificial nucleases are still needed.¹⁵ For example, artificial restriction enzyme can be made sequence specific by encoding sequence specificity into the cleavage agent or by linking it to an appropriate DNA binding agent.¹⁵ Such enzymes are not only very useful for molecular biological field such as DNA cutting at a site not recognized by current restriction enzymes, but also for genomic analysis. In addition, artificial nucleases can be synthesized in large amounts¹⁶ and are often used to elucidate the precise role of active metal ions in natural nucleases.¹⁵ The metal ion accelerates the hydrolysis process by activation of the phosphodiester bond, activation and/or delivery of the nucleophile, and by stabilization of the pentacoordination transition state and the leaving group.^{17,18}

In this study we explore the phosphoesterase activity of ZrK 2 : 2 towards the RNA model system HPNP, a stable phosphodiester characterized by a half-life of hundreds of days at pH 8.0 and 30 °C.¹⁹ As a previous study showed that the solution speciation of this POM is highly dependent on several factors

such as pD, temperature, initial concentration, ionic strength and substrate concentration,¹² the speciation behavior of ZrK 2 : 2 at the conditions used to study HPNP hydrolysis was studied in detail. These results are needed to understand the kinetic experiments and to propose a mechanism for HPNP hydrolysis in the presence of ZrK 2 : 2 POM.

Results and discussion

Aqueous study of ZrK 2 : 2

Depending on the pD, temperature, reaction time, starting concentration, and ionic strength, ZrK 2 : 2 having a single ³¹P resonance at -13.49 ppm²⁰ (Fig. 1a) can convert into the catalytically less active ZrK 1 : 2 (Fig. 1b), characterized by two ³¹P resonances at -14.67 and -14.77 ppm.^{12,21,22} However, recent ³¹P DOSY study on a 3.0 mM aqueous solution of ZrK 2 : 2 also showed the presence of the 1 : 1 Zr^{IV}-substituted Keggin type species (Fig. 1c) with a ³¹P resonance at -13.7 ppm. More importantly, the DFT calculations identified this species as the active species responsible for phosphoester bond hydrolysis in BNPP at pD 6.4 and 60 °C.⁶ Therefore, the aim of this aqueous solution study is to further optimize reaction conditions in such a way that the ZrK 1 : 1 concentration is increased and to apply these conditions to determine the kinetics of HPNP hydrolysis in the presence of ZrK 2 : 2. To the best of our knowledge the synthesis and isolation of pure ZrK 1 : 1 at neutral pD conditions has not been reported. ZrK 1 : 1 is only present as a single species in acidic solutions (pH ≤ 3.4),⁶ while the monolacunary Keggin species, a precursor of ZrK 1 : 1, only exists at near-neutral pH.²³

The effect of pD on the solution behaviour of 1.0 mM ZrK 2 : 2 was recently reported. It was concluded that ZrK 2 : 2 and ZrK 1 : 1 are present in equilibrium in solutions with pD of 5.4 and 6.4. At pD values higher than 6.4, the dominant species is ZrK 2 : 2, while at pD values lower than 5.4, the dominant species is ZrK 1 : 1.⁶ In this study the effect of temperature on the speciation equilibria was determined at nearly neutral pD (pD 6.4).

A ZrK 2 : 2 solution was kept at temperatures ranging from 37 °C to 80 °C, before assessing its species distribution by ³¹P NMR. Fig. S1† shows that both ZrK 2 : 2 (-13.49 ppm)¹² and ZrK 1 : 1 (-13.7 ppm)⁶ are present after mixing for 1 h without heating. Unfortunately, partial overlap of the ZrK 1 : 2 and ZrK 1 : 1 resonances makes integration and therefore quantification difficult. Temperature has no significant effect on the speciation of ZrK 2 : 2 after heating for 1 h up to 60 °C. From 70 °C upward only minor amounts (19%) of ZrK 1 : 2 were detected, ZrK 1 : 1 is present up to 70 °C, and at 80 °C its intensity decreases significantly.

To further observe the influence of concentration and incubation time on the ZrK 1 : 1 species distribution, a 1.0 mM and 3.0 mM solution of ZrK 2 : 2 at pD 6.4 were kept at 50 °C for a prolonged period of time. Fig. S2† indicates that for 1.0 mM of ZrK 2 : 2 both ZrK 2 : 2 and ZrK 1 : 1 were detected after mixing and ZrK 1 : 1 was still present in the solution after heating for

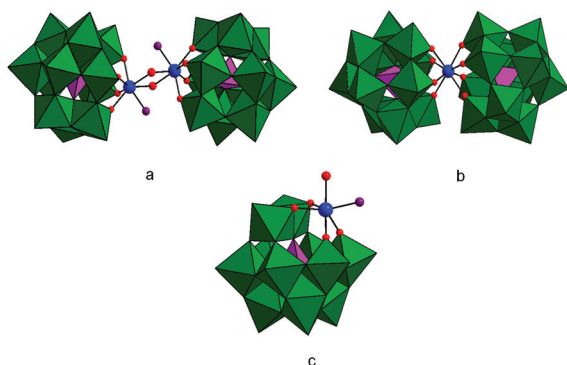


Fig. 1 Structures of ZrK 2 : 2 (a), ZrK 1 : 2 (b) and ZrK 1 : 1 (c). The WO₆ groups are represented by green octahedra, while the internal PO₄ groups are represented by pink tetrahedra. Zr(IV), H₂O molecules and OH group are represented by blue, violet and red balls respectively.



7 h. For a 3.0 mM ZrK 2:2 solution it can be seen from Fig. S3† that no ZrK 1:1 was detected after mixing and after 2 h 25 min, a very small amount of ZrK 1:1 was observed.

Previous studies show that ionic strength has an effect on the POM solution behavior and/or the hydrolysis rate of different molecules such as NPP, BNPP and dipeptide.^{10,12,24,25} Therefore, the influence of ionic strength on the ZrK 1:1 species distribution was also studied for a 1.0 mM sample of ZrK 2:2. ³¹P NMR spectra of a 1.0 mM solution of ZrK 2:2 in the presence of increasing concentrations (0.25 M to 2.0 M) of NaClO₄ at pD 6.4 were recorded after mixing. Fig. S4† shows that an addition of 0.25 M NaClO₄ lead to the disappearance of ZrK 1:1 signal while the signals of ZrK 2:2 and ZrK 1:2 were clearly detected. This means that NaClO₄ can promote the conversion of ZrK 1:1 into ZrK 2:2 or ZrK 1:2^{12,26,27} and higher concentrations of NaClO₄ favoured the conversion of ZrK 2:2 into ZrK 1:2.

In this study, the influence of the substrate HPNP and the inhibitor disodium diphenyl phosphate (DPP) on the equilibria between the different Zr^{IV}-substituted Keggin type POMs was also examined. The concentration of ZrK 2:2 was kept constant (1.0 mM) and the concentration of HPNP was increased from 1.0 mM to 50.0 mM. As can be seen from Fig. S5,† an increase in HPNP concentration lead to the gradual disappearance of ZrK 1:1 and promoted the conversion of ZrK 2:2 into ZrK 1:2. The same trend was seen when using DPP in the concentration range 1.0 mM to 40.0 mM (Fig. S6†). These experiments suggest that the interaction of ZrK 2:2 with HPNP and DPP ligands also plays an important role in the ZrK 1:1 species distribution.

The above results show that most ZrK 1:1 was observed using a 1.0 mM solution of ZrK 2:2 in the absence of salt at pD 6.4 and 50 °C. Therefore, these conditions will be used in the kinetic studies of HPNP hydrolysis.

Hydrolysis of HPNP in the presence of ZrK 2:2

The hydrolysis of HPNP in the presence of ZrK 2:2 (Scheme 1) is conveniently followed by means of ¹H NMR spectroscopy. P–O bond hydrolysis can be observed by the disappearance of the aromatic resonances of HPNP (8.28 ppm and 7.38 ppm) and the appearance of the aromatic *p*-nitrophenyl (NP) resonances at 8.19 ppm and 6.96 ppm. Fig. 2 shows an example of the ¹H NMR spectra for HPNP hydrolysis in the presence of ZrK 2:2 at different time intervals.

Based on the ¹H NMR integration values from Fig. 2, the percentage of HPNP at different time increments was calculated in order to obtain the observed rate constant, and half-life. The percentage of HPNP and NP as a function of reaction time are shown in Fig. S7† and the natural logarithm of the concentration of NPP as a function of time (Fig. S8†) was fitted to a first-order linear decay function. At pD 6.4 and 50 °C an observed rate constant of $11.5(\pm 0.42) \times 10^{-5} \text{ s}^{-1}$ and half-life of 1.7 h were calculated. The presence of equimolar amounts of ZrK 2:2 resulted in a 530-fold rate acceleration in comparison with the spontaneous hydrolysis of HPNP ($2.17(\pm 0.11) \times 10^{-7} \text{ s}^{-1}$) under the same reaction conditions.

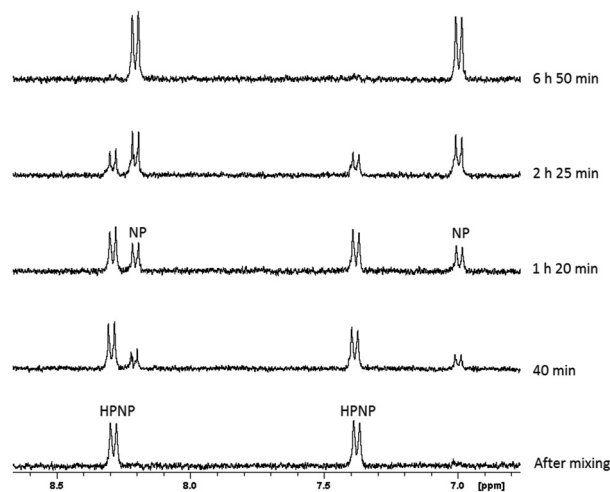


Fig. 2 ¹H NMR of the hydrolysis reaction of 1.0 mM of HPNP in the presence of 1.0 mM of ZrK 2:2 at different time intervals at pD 6.4 and 50 °C.

³¹P NMR spectra (Fig. 3) recorded during the course of the reaction show that cyclic phosphate (CycP), with a ³¹P resonance at 18 ppm, is formed.^{19,28} At the end of hydrolysis, no HPNP resonances were detected in both ¹H and ³¹P NMR spectra, indicating full conversion of HPNP into cyclic phosphate and NP.

Several control experiments were performed. At pD 6.4 and 50 °C, the reaction between HPNP and the monolacunary Keggin POM ([α -PW₁₁O₃₉]⁷⁻) did not show any change in observed rate constant when compared to spontaneous HPNP cleavage. This experiment indicates that the monolacunary POM does not promote HPNP hydrolysis and that the

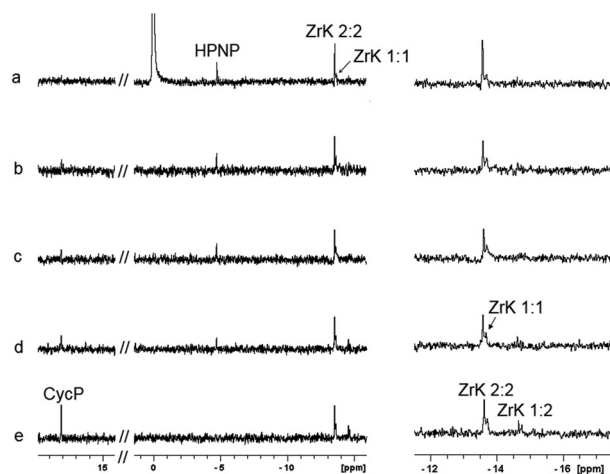


Fig. 3 ³¹P NMR of the hydrolysis reaction between 1.0 mM of HPNP in the presence of 1.0 mM of ZrK 2:2 after (a) mixing, (b) 40 min, (c) 1 h 20 min, (d) 2 h 25 min, (e) 6 h 50 min at pD 6.4 and 50 °C (left) and respectively zoomed upfield region of the spectra (right). (400 MHz, D₂O, 293 K, NS = 1024, 25% H₃PO₄).



embedded Zr(IV) ions are responsible for the observed reactivity. Under identical conditions HPNP hydrolysis promoted by ZrK 1:2 was about 12 times slower ($k_{\text{obs}} = 9.20(\pm 0.56) \times 10^{-6} \text{ s}^{-1}$) in comparison to ZrK 2:2 promoted hydrolysis.

As ZrK 1:2 does not show any conversion into other POM species up to concentrations of 6.0 mM (pD 6.4 and 60 °C),¹² the observed hydrolysis is exclusively the result of the presence of ZrK 1:2. This difference can be explained by the fact that in the case of ZrK 2:2, ZrK 2:2 partially converted into a more active ZrK 1:1 species and this species promoted the reaction resulting in the higher rate constant, while in the case of ZrK 1:2, no ZrK 1:1 species was detected. Under the same conditions, the reaction between the $\text{ZrCl}_2 \cdot 8\text{H}_2\text{O}$ and HPNP was also examined. Under these conditions, the formation of insoluble Zr(IV) hydroxyl polymeric gels^{29,30} was observed, resulting in a rate constant of $2.83(\pm 0.30) \times 10^{-6} \text{ s}^{-1}$. This rate constant represents a 40-fold decrease in comparison to HPNP hydrolysis in the presence of ZrK 2:2.

Effect of pD on HPNP hydrolysis

Since the reactivity and speciation of ZrK 2:2 is strongly affected by pD, the effect of pD on the rate constant of HPNP hydrolysis in the absence and in the presence of ZrK 2:2 was determined in the pD range 4.5 to 9.5. In the absence of ZrK 2:2 at pD 4.5 and 5.5, no hydrolysis of HPNP was observed after 3 months, while in the pD range 6.4 to 9.5, the rate constants are at least two orders of magnitude slower than that in the presence of ZrK 2:2 (Table S1†). The pD-rate constant profile for HPNP hydrolysis in the presence of ZrK 2:2 is bell-shaped, with fastest hydrolysis observed at pD 6.4 (Fig. 4).

This bell-shaped profile further supports a Lewis-acid catalyzed hydrolysis mechanism because if hydrolysis would be Brønsted acid mediated, the rate constants would increase at low pH values. The bell-shaped profile can be explained in the following way. HPNP hydrolysis in the presence of this POM requires OH^- as an active nucleophile and this OH group can

come from either the POM or solvent water molecules.⁶ The deprotonation of water molecules is hindered at pD values smaller than 6.4, resulting in a decrease of k_{obs} at low pD values. The formation of OH^- nucleophiles is facilitated by an increase of pD, leading to a gradual increase of k_{obs} . After reaching a maximum at near neutral pD a decrease of k_{obs} is usually observed due to the formation of a hydrolytically inactive HPNP coordination complex.³¹ ^{31}P NMR shows that during the reaction performed at pD 4.5 (Fig. S9†) only ZrK 1:1 was observed, suggesting that indeed lower reaction rates are not due to the conversion of catalytically more active ZrK 1:1 into ZrK 2:2 or ZrK 1:2, but rather due to the low concentration of OH^- nucleophiles present at low pD. The deprotonation of water nucleophiles as well as the promotion of the conversion of ZrK 2:2 into less active ZrK 1:2 become more evident at pD values higher than 6.4 when k_{obs} of HPNP hydrolysis starts to decrease.

The conversion of ZrK 2:2 into ZrK 1:2 during the course of reaction was evidenced in the reaction mixtures studied at different pD values and 50 °C. Fig. 3 shows that only 11% of ZrK 1:2 was observed after 2 h 25 min at pD 6.4, while in highly alkaline solutions (pD 9.5) further decomposition of ZrK 2:2 into the hydrolytically inactive monolacunary species was observed immediately after mixing (Fig. S10†), resulting in a complete loss of catalytic activity.

Effect of temperature on HPNP hydrolysis

As the temperature also influences the ZrK 2:2 solution equilibria, the effect of temperature on the hydrolysis reaction rate was examined on a solution containing equimolar amounts of HPNP and ZrK 2:2 (1.0 mM) at pD 6.4 in the temperature range from 37 °C to 80 °C. From the data shown in Fig. S11a,† the activation energy ($63.35 \pm 1.82 \text{ kJ mol}^{-1}$) was calculated from the Arrhenius equation, which is significantly lower than the one in the absence of ZrK 2:2 under identical reaction conditions ($131.64 \pm 2.73 \text{ kJ mol}^{-1}$).

Based on the Eyring equation (Fig. S11b†), the enthalpy of activation ($\Delta H^\ddagger = 60.60 \pm 2.09 \text{ kJ mol}^{-1}$) and entropy of activation ($\Delta S^\ddagger = -133.70 \pm 6.13 \text{ J mol}^{-1} \text{ K}$) were calculated. The negative entropy of activation results from the coordination of HPNP to the ZrK POM catalyst. Out of these data, the Gibbs activation energy (ΔG^\ddagger) was calculated to be $102.05 \pm 0.13 \text{ kJ mol}^{-1}$ at 37 °C. This ΔG^\ddagger value is similar to that of BNPP hydrolysis ($111.12 \text{ kJ mol}^{-1}$ at 37 °C) by ZrK 2:2¹² and of NPP hydrolysis ($96.94 \text{ kJ mol}^{-1}$ at 37 °C) by the Wells–Dawson type $\text{K}_{15}\text{H}[\text{Zr}(\alpha_2\text{-P}_2\text{W}_{17}\text{O}_{61})_2] \cdot 25\text{H}_2\text{O}$ POM.⁸

Although ZrK 2:2 speciation studies have shown that high temperatures favor conversion of ZrK 2:2 into ZrK 1:1 and/or ZrK 1:2, the rate of HPNP hydrolysis did increase when the temperature was increased. This result might be explained by the fact that conversion of ZrK 2:2 into ZrK 1:2 is rather slow and ZrK 1:1 is still present during the course of hydrolysis.

Effect of ZrK 2:2 concentration on HPNP hydrolysis

In order to observe the influence of catalyst concentration on the reaction rate, reaction mixtures containing 1.0 mM HPNP

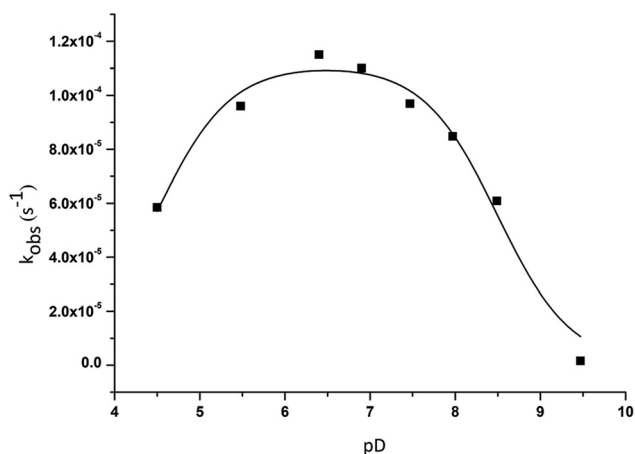
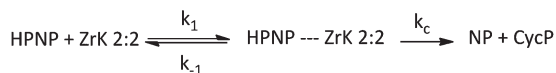


Fig. 4 pD dependence profile of k_{obs} for the cleavage of 1.0 mM of HPNP in the presence of 1.0 mM of ZrK 2:2 at 50 °C.





Scheme 2 General catalytic scheme for HPNP hydrolysis by ZrK 2 : 2.

and increasing amounts of ZrK 2 : 2, ranging from 0.25 mM to 3.0 mM were studied at pD 6.4 and 50 °C. The general catalytic scheme for the hydrolysis of HPNP in the presence of ZrK 2 : 2 is shown in Scheme 2.

Assuming that the formation of the products (k_c) is much slower than reaching the equilibrium between HPNP and ZrK 2 : 2, we have $k_1 + k_{-1} \gg k_c$. Because the formation of nitrophenol (NP) is a first-order reaction, k_{obs} can be written as in eqn (1).^{8,10,11,31}

By fitting the data to eqn (1), the binding constant ($K_f = k_1/k_{-1} = 455 \text{ M}^{-1}$) and the catalytic rate constant ($k_c = 42 \times 10^{-5} \text{ s}^{-1}$) were obtained (Fig. 5). From this figure it is evident that the POM can hydrolyse an excess of HPNP. Complete hydrolysis of HPNP was still observed when 1.0 mM of HPNP and 0.25 mM of ZrK 2 : 2 were used. This suggests that one equivalent of ZrK 2 : 2 hydrolyses at least 4 equivalents of HPNP, demonstrating its catalytic activity.

$$k_{\text{obs}} = \frac{k_c [\text{ZrK } 2:2]_0}{k_{-1}/k_1 + [\text{ZrK } 2:2]_0} \quad (1)$$

Fig. 5 shows that an increase in ZrK 2 : 2 concentration leads to an increase in reaction rate. Despite the fact that higher initial concentrations of ZrK 2 : 2 result in a more favorable conversion to ZrK 1 : 2,¹² the total molar amount of ZrK 2 : 2 in solution is still much higher, resulting in faster hydrolysis. For example, for a 0.5 mL mixture containing 1.0 mM of HPNP and 0.25 mM of ZrK 2 : 2 (0.13×10^{-6} mole), no signal of ZrK 1 : 2 was detected during the course of reaction (Fig. S12†). Fig. 3 shows that a 0.5 mL mixture of 1.0 mM of HPNP and 1.0 mM of ZrK 2 : 2 contains 81% of ZrK 2 : 2 after 2 h 25 min, resulting in 0.43×10^{-6} mole of ZrK 2 : 2. Similarly, when 3.0 mM

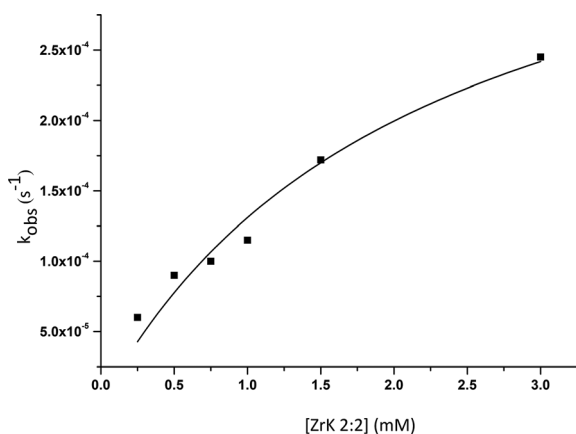


Fig. 5 Dependence of the observed rate constant on the concentration of ZrK 2 : 2 for the hydrolysis of 1.0 mM of HPNP at pD 6.4 and 50 °C.

of ZrK 2 : 2 were used the conversion to ZrK 1 : 2 was larger and 71% of ZrK 2 : 2 was present after 2 h 25 min (Fig. S13†), leading to 1.06×10^{-6} mole of ZrK 2 : 2 present in solution.

Effect of ionic strength on HPNP hydrolysis

Since both ZrK 2 : 2 and HPNP are negatively charged at pD 6.4, the influence of ionic strength on HPNP hydrolysis was examined by adding stepwise NaClO_4 to a mixture containing 1.0 mM of HPNP and 1.0 mM of ZrK 2 : 2. From Fig. S14,† a significant decrease of the rate constant was observed upon adding increasing amounts of NaClO_4 . As above control experiments with the monolacunary Keggin POM ($[\alpha\text{-PW}_{11}\text{O}_{39}]^{7-}$) showed that Zr^{IV} is required factor for the catalytic activity, it is very likely that the binding between HPNP and POM occurs *via* coordination between the negatively charged oxygen of phosphate group of HPNP and the positively charged Zr^{IV} of POM. Addition of salt may hinder this interaction, leading lower reaction rates. However, NaClO_4 also promotes conversion of ZrK 2 : 2 into ZrK 1 : 2 as can be seen from Fig. S15, S16 and S17.† Fig. S15† shows that at pD 6.4, 26% of ZrK 1 : 2 is detected in a reaction mixture containing 0.25 M NaClO_4 , while in the presence of 1.0 M NaClO_4 (Fig. S16†) 70% of ZrK 1 : 2 was observed. When the concentration of NaClO_4 was increased up to 2.0 M (Fig. S17†), full conversion of ZrK 2 : 2 into ZrK 1 : 2 was observed immediately after mixing. From these experiments, it is concluded that NaClO_4 not only plays a role in the binding between HPNP and ZrK 2 : 2, but also in the speciation of this POM in the reaction mixture.

Inhibition study

As DPP is not hydrolyzed after 4 months both in the absence and in the presence of 1.0 mM of ZrK 2 : 2 at pD 6.4 and 60 °C,¹² it is a good candidate for inhibitor studies. The hydrolysis of 1.0 mM of HPNP was followed in the presence of 1.0 mM of ZrK 2 : 2 and increasing amounts from 1.0 mM to 40 mM of DPP. As it can be seen from Fig. S18,† the rate constant of HPNP hydrolysis significantly decreased upon adding increasing amounts of DPP. DPP has a negative effect, as on the one hand it competes with HPNP for the binding to Zr^{IV} and on the other hand it largely shifts equilibrium toward the formation of ZrK 1 : 2, resulting in reaction rate decrease.

Binding between HPNP and ZrK 2 : 2 by ^{31}P NMR

The interaction between HPNP and ZrK 2 : 2 was studied by ^{31}P NMR. At pD 6.4 (Fig. S19†) ZrK 2 : 2 is characterized by a peak at -13.49 ppm, while the HPNP signal can be found at -4.61 ppm (half-width 2.30 Hz). In the presence of 1.0 mM of ZrK 2 : 2 the peak of HPNP is shifted by 0.14 ppm and the half-width increased to 5.14 Hz (Fig. 6). Both the change in chemical shift and the line-broadening support that interaction between HPNP and ZrK 2 : 2 takes place.

Kinetic isotope effect on HPNP hydrolysis and proposed mechanism

The kinetic solvent deuterium isotope effect is a powerful tool for mechanistic studies and gives information on the proton



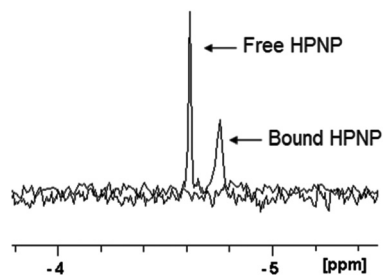


Fig. 6 ^{31}P NMR spectra of 1.0 mM of HPNP and the mixture of 1.0 mM of HPNP and 1.0 mM of ZrK 2 : 2 after adjusting the pD to 6.4 (400 MHz, D_2O , 293 K, NS = 1024, 25% H_3PO_4).

transfer processes in or before the rate-limiting step of the reaction.³² RNA model phosphate diesters can be hydrolysed by two possible mechanisms that can be distinguished by examining the influence of H_2O or D_2O as a solvent on the kinetics of hydrolysis. When the solvent deuterium kinetic isotope effect (skie), characterized by the $k_{\text{H}_2\text{O}}/k_{\text{D}_2\text{O}}$ ratio, is lower than 1.5 a nucleophilic mechanism is expected. At skie ratios higher than 2 the reaction proceeds *via* a general base mechanism.^{28,33}

In order to propose a mechanism for HPNP hydrolysis, the skie was calculated. The reaction rates for 1.0 mM HPNP hydrolysis in the presence of 1.0 mM ZrK 2 : 2 in H_2O or D_2O were calculated at identical conditions (pD 6.4 and 50 °C). The hydrolysis in H_2O proceeded with the rate constant $13.80 (\pm 0.83) \times 10^{-5} \text{ s}^{-1}$, while for the reaction in D_2O a rate constant of $11.50 (\pm 0.42) \times 10^{-5} \text{ s}^{-1}$ was observed. From these results, a skie effect of 1.2 was calculated and this value of skie effect supports the nucleophilic mechanism.^{28,33} ^1H spectra (Fig. 2) show that one of the products of HPNP hydrolysis is nitrophenol and ^{31}P spectra (Fig. 3) show that another product of HPNP hydrolysis is cyclic phosphate with a ^{31}P chemical shift at 18 ppm.^{19,28} From ^{31}P NMR measurements, kinetic experiments and isotope effect study, the mechanism of HPNP hydrolysis in the presence of ZrK 2 : 2 was proposed as following. As already shown in our previous study, under the reaction conditions there is an interconversion between ZrK 2 : 2, ZrK 1 : 1 and/or ZrK 1 : 2.⁶ The Zr atom in the ZrK 1 : 2 species is coordinatively saturated and hardly accessible for the bulky HPNP ligand, as it is sandwiched by the two Keggin moieties. Therefore, HPNP coordination to ZrK 1 : 2 is not expected.⁶ ZrK 1 : 1 was found to be more catalytically active when compared to ZrK 2 : 2 as its Zr(IV) ion has more coordinated water molecules that can be replaced by the substrate or that can act as a nucleophile.⁶ We suggest that ZrK 1 : 1 can act as an active species in this HPNP hydrolytic reaction by coordination to the oxygen atom of the phosphate group of HPNP. This suggestion is experimentally supported by the observed shift and line-broadening of the HPNP signal in the ^{31}P spectrum (Fig. 6). This binding would result in a more positive charge on the phosphorous atom of HPNP, which facilitates the nucleophilic attack of the OH group of ZrK 1 : 1 or from water molecule of

the solvent, thus leading to cleavage of the P–O bond and the formation of nitrophenol and cyclic phosphate.

Conclusions

In summary, we report the first example of the hydrolysis of HPNP promoted by a binuclear Zr(IV)-substituted Keggin type polyoxometalate. ^{31}P NMR measurements offer the evidence that the ZrK 1 : 1 species, which is proposed as the active species, is the major and stable species under the reaction conditions. A 530-fold rate increase in comparison to the blank reaction was observed for HPNP hydrolysis. The present study demonstrates the potential of Zr(IV)-substituted POMs as artificial phosphatase and contributes to the further development of POMs as Lewis acid catalysts for the hydrolysis of biomolecules.^{38–40} The results from this study encourage us to further exploit the hydrolytic activity of this POM towards other more complex substrates such as adenosine triphosphate (ATP), DNA/RNA fragments, pesticides such as paraoxon and parathion, and nerve agents such as soman and sarin.

Experimental

Materials

The Zr-substituted Keggin POMs $(\text{Et}_2\text{NH}_2)_8[\{\alpha\text{-PW}_{11}\text{O}_{39}\text{Zr}(\mu\text{-OH})(\text{H}_2\text{O})\}_2 \cdot 7\text{H}_2\text{O}$ ($\delta = -13.49 \text{ ppm}$)^{20,34} (ZrK 2 : 2), and $(\text{Et}_2\text{NH}_2)_{10}[\text{Zr}(\text{PW}_{11}\text{O}_{39})_2] \cdot 7\text{H}_2\text{O}$ ($\delta = -14.67$ and -14.77 ppm)²¹ (ZrK 1 : 2) as well as 2-hydroxypropyl-4-nitrophenyl phosphate ($\delta = -4.64 \text{ ppm}$)^{35,36} (HPNP) were synthesized and characterized according to literature. Disodium diphenyl phosphate (DPP, $\text{C}_6\text{H}_5\text{PO}_4\text{Na}_2 \cdot 2\text{H}_2\text{O}$), DCl, and NaOD were purchased from Acros and used without any further purification.

Kinetic measurements

Solutions containing 1.0 mM of HPNP and 1.0 mM of ZrK 2 : 2 were prepared in D_2O . The final pD was adjusted with minor amounts of 10% DCl and 15% NaOD solutions in D_2O . The pH-meter value was corrected by using the equation: pD = pH meter reading + 0.41.³⁷ The pD of the samples was measured at the beginning and at the end of hydrolysis, and the difference was typically less than 0.5 units. The reaction mixture was kept at constant temperature and ^1H NMR spectra were measured at certain time intervals during the hydrolytic reaction to calculate the observed rate constant (k_{obs}) by the integral method.

NMR spectroscopy

^1H NMR spectra were recorded on a Bruker Avance 400 and 0.5 mM of 3-(trimethylsilyl)propionic-2,2,3,3-d₄ acid (TMSP) was used as an internal standard. ^{31}P NMR spectra were recorded on a Bruker Avance 400 and Bruker Avance II+ 600 NMR spectrometer using power-gated ^1H decoupling with 30 degree flip angle (zgpg30 pulse programme) and 25% phosphoric acid was used as a ^{31}P external reference.



Acknowledgements

T.N.P-V. and P.S. (BOF + fellowship) thank KU Leuven for the financial support and F. W. O. Flanders for a bilateral project. T.K.N.L. thanks the Vietnamese Government and KU Leuven for a doctoral fellowship. G.A. thanks F. W. O. Flanders for a post-doctoral fellowship. The authors acknowledge the CMST COST Action CM1203 (Polyoxometalate Chemistry for Molecular Nanoscience) for the financial support in terms of STSM applications.

Notes and references

- M. Carraro and S. Gross, *Materials*, 2014, **7**, 3956–3989.
- A. Proust, B. Matt, R. Villanneau, G. Guillemot, P. Gouzerh and G. Izzet, *Chem. Soc. Rev.*, 2012, **41**, 7605–7622.
- H. Stephan, M. Kubeil, F. Emmerling and C. E. Müller, *Eur. J. Inorg. Chem.*, 2013, **2013**, 1585–1594.
- N. V. Izarova, M. T. Pope and U. Kortz, *Angew. Chem., Int. Ed.*, 2012, **51**, 9492–9510.
- A. Sartorel, M. Bonchio, S. Campagna and F. Scandola, *Chem. Soc. Rev.*, 2013, **42**, 2262–2280.
- T. K. N. Luong, P. Shestakova, T. T. Mihaylov, G. Absillis, K. Pierloot and T. N. Parac-Vogt, *Chem. – Eur. J.*, 2015, **21**, 4428–4439.
- P. Nunes, A. C. Gomes, M. Pillinger, I. S. Gonçalves and M. Abrantes, *Microporous Mesoporous Mater.*, 2015, **208**, 21–29.
- S. Vanhaecht, G. Absillis and T. N. Parac-Vogt, *Dalton Trans.*, 2012, **41**, 10028–10034.
- N. Steens, A. M. Ramadan, G. Absillis and T. N. Parac-Vogt, *Dalton Trans.*, 2010, **39**, 585–592.
- G. Absillis, R. van Deun and T. N. Parac-Vogt, *Inorg. Chem.*, 2011, **50**, 11552–11560.
- E. Cartuyvels, G. Absillis and T. N. Parac-Vogt, *Chem. Commun.*, 2008, 85–87.
- T. K. N. Luong, G. Absillis, P. Shestakova and T. N. Parac-Vogt, *Eur. J. Inorg. Chem.*, 2014, **2014**, 5276–5284.
- D. M. Perreault and E. V. Anslyn, *Angew. Chem., Int. Ed. Engl.*, 1997, **36**, 432–450.
- M. Oivanen, S. Kuusela and H. Lönnberg, *Chem. Rev.*, 1998, **98**, 961–990.
- E. L. Hegg and J. N. Burstyn, *Coord. Chem. Rev.*, 1998, **173**, 133–165.
- D. T. Thomas, in *Metal-DNA Chemistry*, American Chemical Society, 1989, ch. 1, vol. 402, pp. 1–23.
- D. E. Wilcox, *Chem. Rev.*, 1996, **96**, 2435–2458.
- N. Sträter, W. N. Lipscomb, T. Klabunde and B. Krebs, *Angew. Chem., Int. Ed. Engl.*, 1996, **35**, 2024–2055.
- H. Arora, S. K. Barman, F. Lloret and R. Mukherjee, *Inorg. Chem.*, 2012, **51**, 5539–5553.
- K. Nomiya, Y. Saku, S. Yamada, W. Takahashi, H. Sekiya, A. Shinohara, M. Ishimaru and Y. Sakai, *Dalton Trans.*, 2009, 5504–5511.
- C. N. Kato, A. Shinohara, K. Hayashi and K. Nomiya, *Inorg. Chem.*, 2006, **45**, 8108–8119.
- L. Cai, Y. Li, C. Yu, H. Ji, Y. Liu and S. Liu, *Inorg. Chim. Acta*, 2009, **362**, 2895–2899.
- S. Himeno, M. Takamoto and T. Ueda, *Bull. Chem. Soc. Jpn.*, 2005, **78**, 1463–1468.
- P. H. Ho, E. Breynaert, C. E. A. Kirschhock and T. N. Parac-Vogt, *Dalton Trans.*, 2011, **40**, 295–300.
- P. H. Ho, T. Mihaylov, K. Pierloot and T. N. Parac-Vogt, *Inorg. Chem.*, 2012, **51**, 8848–8859.
- C. Zhang, R. C. Howell, Q.-H. Luo, H. L. Fieselmann, L. J. Todaro and L. C. Francesconi, *Inorg. Chem.*, 2005, **44**, 3569–3578.
- C. Zhang, L. Bensaid, D. McGregor, X. F. Fang, R. C. Howell, B. Burton-Pye, Q. H. Luo, L. Todaro and L. C. Francesconi, *J. Cluster Sci.*, 2006, **17**, 389–425.
- L. Bonfá, M. Gatos, F. Mancin, P. Tecilla and U. Tonellato, *Inorg. Chem.*, 2003, **42**, 3943–3949.
- A. Singhal, L. M. Toth, J. S. Lin and K. Affholter, *J. Am. Chem. Soc.*, 1996, **118**, 11529–11534.
- R. A. Moss, J. Zhang and K. G. Ragunathan, *Tetrahedron Lett.*, 1998, **39**, 1529–1532.
- J. H. Espenson, *Chemical kinetics and reaction mechanisms*, McGraw-Hill, New York, 1994.
- N. Virtanen, L. Polari, M. Vällilä and S. Mikkola, *J. Phys. Org. Chem.*, 2005, **18**, 385–397.
- C. Maxwell, A. A. Neverov and R. S. Brown, *Org. Biomol. Chem.*, 2005, **3**, 4329–4336.
- H. G. T. Ly, G. Absillis and T. N. Parac-Vogt, *Dalton Trans.*, 2013, **42**, 10929–10938.
- D. M. Brown and D. A. Usher, *J. Chem. Soc.*, 1965, 6558–6564.
- J. S. W. Tsang, A. A. Neverov and R. S. Brown, *J. Am. Chem. Soc.*, 2003, **125**, 1559–1566.
- P. K. Glasoe and F. A. Long, *J. Phys. Chem.*, 1960, **64**, 188–190.
- K. Stroobants, G. Absillis, E. Moelants, P. Proost and T. N. Parac-Vogt, *Chem. – Eur. J.*, 2014, **20**, 3894–3897.
- K. Stroobants, V. Goovaerts, G. Absillis, G. Bruylants, E. Moelants, P. Proost and T. N. Parac-Vogt, *Chem. – Eur. J.*, 2014, **20**, 9567–9577.
- H. G. T. Ly, G. Absillis, R. Janssens, P. Proost and T. N. Parac-Vogt, *Angew. Chem.*, 2015, **127**, 7499.

